INTEGRATED ORBIT AND ATTITUDE CONTROL FOR A NANOSATELLITE WITH POWER CONSTRAINTS

Bo J. Naasz,* Matthew M. Berry,† Hye-Young Kim,‡
and Christopher D. Hall§

Small satellites tend to be power-limited, so that actuators used to control the orbit and attitude must compete with each other as well as with other subsystems for limited electrical power. The Virginia Tech nanosatellite project, HokieSat, must use its limited power resources to operate pulsed-plasma thrusters for orbit control and magnetic torque coils for attitude control, while also providing power to a GPS receiver, a crosslink transceiver, and other subsystems. The orbit and attitude control strategies were developed independently. The attitude control system is based on an application of LQR to an averaged system of equations, whereas the orbit control is based on orbit element feedback. In this paper we describe the strategy for integrating these two control systems and present simulation results to verify the strategy.

INTRODUCTION

The concept of orbit and attitude coupling has received little attention in the literature. The time scales of these two systems usually differ enough that the orbit can be considered as given when considering attitude dynamics. In some cases, however, this assumption is unwise, and consideration must be given to the coupling of the translational and rotational systems. Integration of spacecraft orbit and attitude subsystems is motivated by a variety of concepts including natural system dynamics, and guidance, navigation and control (GNC) system issues such as shared resources, subsystem inter-dependencies, and actuator-induced disturbances.

Natural coupling of rotation and translation is apparent in such concepts as variation of atmospheric drag and solar radiation pressure as a function of attitude-dependent cross-sectional areas, variation of magnetic and gravity gradient torques as a function of both

*Formerly Graduate Research Assistant. Currently with NASA Goddard Space Flight Center, Flight Dynamics Analysis Branch, Code 572 Greenbelt, MD 20771, (301) 286-3819, bo.j.naasz@nasa.gov

†Graduate Research Assistant, Aerospace and Ocean Engineering, Virginia Polytechnic Institute and State University, Blacksburg, Virginia. maberry2@vt.edu

‡Post-doctoral Research Assistant, Aerospace and Ocean Engineering, Virginia Polytechnic Institute and State University, Blacksburg, Virginia. hyekim@vt.edu

§Associate Professor,Aerospace and Ocean Engineering, Virginia Polytechnic Institute and State University, Blacksburg, Virginia. Associate Fellow AIAA. Member AAS. cdhall@vt.edu. voice (540) 231-2314. fax (540) 231-9632

attitude and orbit position, and dynamical coupling of orbit and attitude dynamics (a weak effect which is most often negligible).[1,2]

There are numerous examples of shared resources, including shared actuators (thrusters for orbit and attitude control, as well as for momentum dumping maneuvers), shared sensors (optical systems for attitude determination and celestial navigation), and other shared resources such as power and spacecraft consumables. Subsystem inter-dependencies include, for example, the dependence of the orbit control system (OCS) on the attitude control system (ACS) for actuator pointing. This concept is especially important for spacecraft employing atmospheric drag or solar radiation pressure control techniques. Actuator-induced disturbances include effects such as torques and forces induced by the use of non-coupled or misaligned thrusters to perform rotational or translational maneuvers. This concept also introduces the need for cooperation between attitude and orbit control and determination subsystems to support accurate state estimation.

In this paper, we explore some of these orbit-attitude integration issues as applicable to the HokieSat spacecraft.[3] The spacecraft is one of three small spacecraft in the Ionospheric Observation Nanosatellite Formation (ION-F).[4] The overall configuration and structural design of the satellite is described in Refs. 5 and 6. The attitude control system, including the hardware configuration and the algorithm development, is described in Refs. 7, 8, and 9. The orbit control system is described in Refs. 10, 11, and 12, and related optimal control concepts are described in Refs. 13 and 14.

MISSION DESCRIPTION AND HARDWARE CONSTRAINTS

HokieSat is a small spacecraft being built by students at Virginia Tech.[3] The spacecraft, formally known as the Virginia Tech Ionospheric Scintillation Measurement Mission, is part of the Ionospheric Observation Nanosatellite Formation (ION-F) project.[4] The project involves spacecraft built by three schools: Virginia Tech, Utah State University, and Cornell University. The three spacecraft are similar in design and will perform formation flying demonstrations and make ionospheric measurements while in an orbit approximately the same as that of the International Space Station ($i \approx 52°$, $a \approx 6770$ km).

HokieSat is hexagon-shaped, about 0.5 m in major diameter and about 0.3 m tall, with a mass of about 20 kg. The spacecraft uses Pulsed Plasma Thrusters (PPTs) to maintain its position in the formation.[15,16] There are two pairs of PPTs on HokieSat; their position on the hexagonal cross-section is shown in Fig. 1. Thrusters T_2 and T_3 provide translation control, and Thrusters T_1 and T_4 can provide yaw steering, or can provide translation control. Each thruster can be fired individually. However because they share a capacitor, thrusters T_1 and T_2 or thrusters T_3 and T_4 cannot be fired simultaneously. Thrusters T_2 and T_3 can be fired simultaneously, as can thrusters T_1 and T_4. Each thruster provides an impulse-bit of 56 μN-s and fires at a rate of 1 Hz. For translation control thrusters T_2 and T_3 are fired together providing an impulse-bit of 112 μN-s. All four thrusters are positioned slightly above the center of mass, and therefore exert a small pitch or roll torque on the spacecraft. There are no thrusters in the zenith-nadir directions, and the communication system requires that the spacecraft remain nadir-pointing; thus there is no way to thrust in the radial direction.

Attitude is controlled by three orthogonal magnetic torque coils.[7,8] Attitude control is achieved by forcing a current through the torque coils, thereby generating a net magnetic

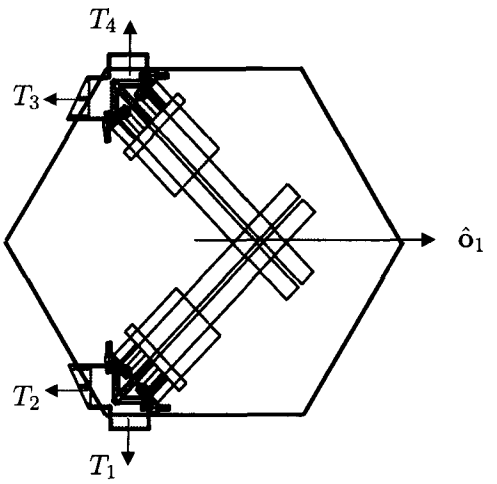

Figure 1: HokieSat pulsed plasma thruster (PPT) layout viewed from zenith direction

moment which interacts with the Earth's magnetic field and creates a torque. Due to magnetic field interactions between the coils and the PPTs, the two actuator systems cannot be used simultaneously, and any attitude or orbit control must be performed in a piecewise fashion. Power limitations place an additional constraint on the control system. When the spacecraft is in eclipse, the power subsystem can provide only enough power to operate vital spacecraft functions; therefore, attitude control can be accomplished during eclipse, whereas orbit control can only be accomplished when the spacecraft is in sunlight.

HokieSat's nominal flight orientation is nadir pointing, with thrusters T_2 and T_3 pointing opposite the velocity vector (see Figure 1). The most obvious control mode employs torque coils to slew the spacecraft as required to point thrusters T_2 and T_3 in the direction dictated by the orbit control law. This mode is termed the "normal" control mode. A less obvious control strategy is to turn the spacecraft sideways, so that thrusters T_2 and T_3 point in the negative orbit normal direction, with thruster T_1 and T_4 aligned with the velocity and negative velocity directions. This mode is termed the "sideways" control mode.

The normal control mode benefits from two parallel thrusters (and thus doubled ΔV), and no thrust torque disturbance about the yaw axis. The primary disadvantage is the inherent requirement that the attitude control system perform 180° slew maneuvers whenever the requested thrust vector changes directions. We can modify the orbit control law to discourage this thrust vector flipping by recognizing that all elements except the semi-major axis (and thus the true anomaly) can be controlled without thrust vector flipping. For example, positive changes in the inclination are created by thrusting in the orbit normal direction when the spacecraft is above the equator. If negative changes are required, the control law can simply wait for the spacecraft to move below the equator, where thrust in the orbit normal direction results in negative inclination change. This observation is useful. Unfortunately, there is no way to force positive and negative semi-major axis changes without applying thrust in opposing directions (the positive and negative velocity vector directions), and large slew maneuvers are unavoidable for the normal control mode.

The sideways control mode benefits from the fact that thrust is readily available in the positive and negative velocity directions, as well as one out-of-plane direction. The major disadvantage of the sideways control mode is the torque induced by orbit control thrusting.

Thrusters T_1 and T_4 are not aligned with the center of mass, and thus create yaw torque about the zenith-nadir directions. This disturbance torque has the same order of magnitude as the torque available from the torque coils. In this control mode, the out-of-plane elements are controlled as described above, with thrust only in the positive orbit normal direction. The sideways control mode requires no large slew maneuvers, but does require attitude control to compensate for the thruster disturbance torque.

Reference 10 described various linear and nonlinear control laws for HokieSat to maintain the formation. These orbit control laws include the non-radial thrust constraint, and the constraint on the thrust magnitude. The control laws assume that the necessary attitude can be achieved instantaneously, and that there is no power constraint. Reference 7 described an LQR-based attitude control for the HokieSat mission. The control law was developed to maintain nadir-pointing, but not to perform yaw-steering for thruster pointing. The control law did not enforce any power constraints on torque coil operations.

The coupling of these power-constrained orbit and attitude control laws is an interesting nonlinear control problem. Interruption of the orbital control may drive the system unstable. In this paper, we implement integrated nonlinear orbit and attitude control laws and test their performance in a realistic formation simulation.

EQUATIONS OF MOTION

In this section we describe the system dynamics models used in verification of the control strategies.

Keplerian Orbital Dynamics

In cartesian form, the equations of motion for a point-mass satellite take the form

$$\ddot{\vec{\mathbf{r}}} = -\frac{\mu}{\|\vec{\mathbf{r}}\|^3}\vec{\mathbf{r}} + \vec{\mathbf{a}}_p \tag{1}$$

where $\vec{\mathbf{r}}$ is the position vector of the satellite measured from the center of mass of the primary body, μ is the gravitational parameter of that body, and $\vec{\mathbf{a}}_p$ includes perturbation accelerations caused by oblateness effects of the body, atmospheric drag, third body effects and so on. If $\vec{\mathbf{a}}_p = \mathbf{0}$ then the equations of motion reduce to the ideal Keplerian situation where the body is a perfect sphere and all other disturbances are zero.

We use the Earth-centered inertial frame, $\mathcal{F}_i$, with the $\hat{\mathbf{i}}_3$-axis aligned with the north pole, the $\hat{\mathbf{i}}_1$-axis aligned with the equinox direction through the equatorial plane, and the $\hat{\mathbf{i}}_2$-axis completing the orthonormal set. We also refer to the spacecraft orbital frame, $\mathcal{F}_o$, which is centered on the spacecraft, with the $\hat{\mathbf{o}}_3$-axis aligned with the vector from the spacecraft to the center of the Earth, the $\hat{\mathbf{o}}_2$-axis aligned with the negative orbit normal direction, and the $\hat{\mathbf{o}}_1$-axis aligned with the velocity direction for circular orbits. The spacecraft body frame, $\mathcal{F}_b$, is centered on and fixed to the spacecraft. The $\hat{\mathbf{b}}_1$-axis is in the normal mode thrust direction (the direction opposite thrusters T_2 and T_3), the $\hat{\mathbf{b}}_3$ direction points through the nadir panel, and the $\hat{\mathbf{b}}_2$ direction completes the right-hand set.

We define the classical orbital elements as semi-major axis, a, eccentricity, e, inclination, i, right ascension of the ascending node, Ω, argument of periapse, ω, and mean anomaly,

M. The first five orbital elements describe the size, shape, and orientation of the orbit in inertial space. The final element describes the spacecraft's angular position within the orbit, referenced from periapse, and has constant angular rate given by the mean motion, n. The equations of motion of a controlled spacecraft in terms of the classical orbital element set are given by Gauss's form of Lagrange's planetary equations:[17]

$$\frac{da}{dt} = \frac{2a^2}{h}\left(e\sin\nu\, u_r + \frac{p}{r}\, u_\theta\right) \tag{2}$$

$$\frac{de}{dt} = \frac{1}{h}\left\{p\sin\nu\, u_r + [(p+r)\cos\nu + re]\, u_\theta\right\} \tag{3}$$

$$\frac{di}{dt} = \frac{r\cos\theta}{h} u_h \tag{4}$$

$$\frac{d\Omega}{dt} = \frac{r\sin\theta}{h\sin i} u_h \tag{5}$$

$$\frac{d\omega}{dt} = \frac{1}{he}\left[-p\cos\nu\, u_r + (p+r)\sin\nu\, u_\theta\right] - \frac{r\sin\theta\cos i}{h\sin i} u_h \tag{6}$$

$$\frac{dM}{dt} = n + \frac{b}{ahe}\left[(p\cos\nu - 2re)u_r - (p+r)\sin\nu\, u_\theta\right] \tag{7}$$

where u_r, u_θ, and u_h are the radial, transverse, and orbit normal control acceleration components, ν is the true anomaly, $\theta = \omega + \nu$ is the argument of latitude, and b, h, and p are the semi-minor axis, the angular momentum, and the semi-latus rectum, respectively.

Attitude Dynamics

We use Euler parameters, or quaternions, to describe the spacecraft attitude. The quaternion, $\overline{\mathbf{q}}$ is defined in terms of the Euler axis, $\mathbf{a}$, and the Euler angle, Φ:

$$\mathbf{q} = \mathbf{a}\sin\frac{\Phi}{2} \tag{8}$$

$$q_4 = \cos\frac{\Phi}{2} \tag{9}$$

$$\overline{\mathbf{q}} = \begin{bmatrix} \mathbf{q} \\ q_4 \end{bmatrix} \tag{10}$$

The time rate of change of the quaternion is written in terms of the angular velocity, ω, as

$$\dot{\overline{\mathbf{q}}} = \frac{1}{2}\begin{bmatrix} \mathbf{q}^\times + q_4\mathbf{1} \\ -\mathbf{q}^T \end{bmatrix}\omega \tag{11}$$

where $\mathbf{q}^\times$ is the skew symmetric matrix:

$$\mathbf{q}^\times = \begin{bmatrix} 0 & -q_3 & q_2 \\ q_3 & 0 & -q_1 \\ -q_2 & q_1 & 0 \end{bmatrix} \tag{12}$$

The rotational equations of motion for a rigid body, Euler's equations, are

$$\mathbf{I}\dot{\omega} = -\omega^\times\mathbf{I}\omega + \mathbf{g}_e \tag{13}$$

where $\mathbf{I}$ is the moment of inertia matrix, and $\mathbf{g}_e$ is the external torque on the body.

For an orbiting spacecraft, external torques include the control torque, $\mathbf{g}_c$, the gravity gradient torque, $\mathbf{g}_{gg}$, and other lesser torques from atmospheric drag, solar radiation pressure, and other environmental effects. For the simulations presented here, we consider only control torques (both intended and unintended) and gravity gradient torques. The gravity gradient torque is given by

$$\mathbf{g}_{gg} = 3\omega_c^2 \mathbf{o}_3^{\times} \mathbf{I} \mathbf{o}_3 \tag{14}$$

where ω_c is the mean motion (also denoted n).

ATTITUDE CONTROL

The attitude control torque is effected by controlling the current in three mutually orthogonal magnetic torque coils, thereby generating a magnetic moment, $\mathbf{M}$. The resulting torque is $\mathbf{g} = \mathbf{M} \times \mathbf{B}$, where $\mathbf{B}$ is the magnetic field vector. The $\mathbf{B}$ field varies with both orbital and diurnal periods, and it is clearly not possible to cause a torque about the $\mathbf{B}$ direction. Thus, magnetic attitude control is inherently underactuated and involves time-varying parameters. The approach taken in Refs. 7 and 8 was based on linearizing the attitude motion about the nominal nadir attitude, averaging the $\mathbf{B}$ field, and applying LQR to the resulting linearized equations of motion. Subsequent Floquet analysis and nonlinear simulations were used to verify performance of the resulting controller. For further details, see Refs. 7 and 8.

ORBIT CONTROL

The orbital equations of motion $(2-7)$ can be written as:

$$\dot{\mathbf{oe}} = \mathbf{f}(\mathbf{oe}) + \tilde{\mathbf{G}}(\mathbf{oe})\mathbf{u} \tag{15}$$

where $\tilde{\mathbf{G}}(\mathbf{oe})$ is the input matrix, whose elements are evident from Eqs. $(2-7)$. We separate these equations of motion into two systems: one system consisting of the first five elements, which define the shape, size, and orientation of the orbit, and the second system consisting of the in-plane angular position of the spacecraft.

For the first system, we define the elemental error $\boldsymbol{\eta}$ as

$$\boldsymbol{\eta} = \begin{bmatrix} a - a^* \\ e - e^* \\ i - i^* \\ \Omega - \Omega^* \\ \omega - \omega^* \end{bmatrix} = \begin{bmatrix} \delta a \\ \delta e \\ \delta i \\ \delta\Omega \\ \delta\omega \end{bmatrix} \tag{16}$$

where $*$ designates target elements. The equations of motion for this system are:

$$\dot{\boldsymbol{\eta}} = \mathbf{G}\mathbf{u} \tag{17}$$

where $\mathbf{u}$ is the vector control acceleration in radial, transverse, and orbit normal directions,

and the input matrix, $\mathbf{G}$ comprises the first five rows of $\tilde{\mathbf{G}}(\mathbf{oe})$:

$$\mathbf{G} = \begin{bmatrix} \frac{2a^2 e \mathrm{S}\nu}{h} & \frac{2a^2 p}{hr} & 0 \\ \frac{p\mathrm{S}\nu}{h} & \frac{(p+r)\mathrm{C}\nu + re}{h} & 0 \\ 0 & 0 & \frac{r\mathrm{C}(\omega+\nu)}{h} \\ 0 & 0 & \frac{r\mathrm{S}(\omega+\nu)}{hSi} \\ -\frac{p\mathrm{C}\nu}{he} & \frac{(p+r)\mathrm{S}\nu}{he} & -\frac{r\mathrm{S}(\omega+\nu)\mathrm{C}i}{hSi} \\ \frac{b(p\mathrm{C}\nu - 2re)}{ahe} & -\frac{b(p+r)\mathrm{S}\nu}{ahe} & 0 \end{bmatrix} \tag{18}$$

where the sine and cosine functions are abbreviated as $\mathrm{S}(\cdot)$ and $\mathrm{C}(\cdot)$. A candidate Lyapunov function for this system, weighted by positive gains, K_j, is given by

$$V(\boldsymbol{\eta}) = \frac{1}{2}\left[K_a \delta a^2 + K_e \delta e^2 + K_i \delta i^2 + K_\Omega \delta\Omega^2 + K_\omega \delta\omega^2\right] \tag{19}$$

The time derivative of $V(\boldsymbol{\eta})$ is given by

$$\dot{V}(\boldsymbol{\eta}) = \mathbf{V}_\eta \, \dot{\boldsymbol{\eta}} = \mathbf{V}_\eta \, \mathbf{G}(\boldsymbol{\eta})\mathbf{u} \tag{20}$$

where

$$\mathbf{V}_\eta = \begin{bmatrix} K_a \delta a & K_e \delta e & K_i \delta i & K_\Omega \delta\Omega & K_\omega \delta\omega \end{bmatrix} \tag{21}$$

Choosing the control, $\mathbf{u}$, as

$$\mathbf{u} = -\mathbf{G}^T \mathbf{V}_\eta^T \tag{22}$$

results in a negative semi-definite time derivative of V:

$$\dot{V}(\boldsymbol{\eta}) = -\mathbf{V}_\eta \, \mathbf{G}\mathbf{G}^T \mathbf{V}_\eta^T \tag{23}$$

To prove asymptotic stability, we apply LaSalle's invariance theorem. The time derivative of the Lyapunov function is always zero when $\boldsymbol{\eta} = \mathbf{0}$, and could be zero when the trigonometric functions of θ are zero, which occurs when $\theta = k\pi/2$, where k is an integer. The set where $\theta = k\pi/2$ is not an invariant set, because θ is time-varying and therefore trajectories that start in the set do not remain in the set. Therefore, the largest invariant set where $\dot{V} = 0$ is the set $\boldsymbol{\eta} = \mathbf{0}$. By Lyapunov's direct method, and LaSalle's invariance principle, the system is asymptotically stable under the choice of control given in Eq. (24). Furthermore, the system is globally asymptotically stable because $V \to \infty$ as $|\boldsymbol{\eta}| \to \infty$. Thus, the desired feedback control is given by

$$\mathbf{u}_{\mathrm{cl}} = -\mathbf{G}^T \mathbf{V}_\eta^T = -\begin{bmatrix} \frac{2a^2 e \mathrm{S}\nu}{h} & \frac{2a^2 p}{hr} & 0 \\ \frac{p\mathrm{S}\nu}{h} & \frac{(p+r)\mathrm{C}\nu + re}{h} & 0 \\ 0 & 0 & \frac{r\mathrm{C}(\omega+\nu)}{h} \\ 0 & 0 & \frac{r\mathrm{S}(\omega+\nu)}{hSi} \\ -\frac{p\mathrm{C}\nu}{he} & \frac{(p+r)\mathrm{S}\nu}{he} & -\frac{r\mathrm{S}(\omega+\nu)\mathrm{C}i}{hSi} \\ \frac{b(p\mathrm{C}\nu - 2re)}{ahe} & -\frac{b(p+r)\mathrm{S}\nu}{ahe} & 0 \end{bmatrix}^T \begin{bmatrix} K_a & \delta a \\ K_e & \delta e \\ K_i & \delta i \\ K_\Omega & \delta\Omega \\ K_\omega & \delta\omega \end{bmatrix} \tag{24}$$

The angle errors $\delta\Omega$, $\delta\omega$, and δM are measured from parameters defined between 0 and 2π. To ensure proper error feedback, these angular errors should be "short-way" angle measurements, defined between $-\pi$ and π.

Mean Motion Control

To control the in-plane angular motion of the spacecraft, we take advantage of a useful natural component of the nonlinear dynamics: the differential mean motion, δn. Observe that an effective method for correcting in-track errors is to force a semi-major axis error, changing the mean motion such that the in-plane angle is corrected. For an uncontrolled spacecraft in two-body motion, the orbital element dynamics simplify to

$$\frac{dM}{dt} = n \tag{25}$$

and thus the relative dynamics can be written as

$$\frac{d}{dt}(\delta M) = \frac{dM}{dt} - \frac{dM^*}{dt} = n - n^* = \delta n \tag{26}$$

where

$$\delta n = \sqrt{\frac{\mu}{a^3}} - \sqrt{\frac{\mu}{a^{*3}}} \tag{27}$$

To drive the mean anomaly error, δM, to zero, we use

$$\delta \dot{M} = -K_n \delta M \tag{28}$$

where K_n is a positive gain. Combining Eqs. (27) and (28), and using canonical units ($\mu = 1$), we obtain

$$-K_n \delta M = \sqrt{\frac{1}{a^3}} - \sqrt{\frac{1}{a^{*3}}} \tag{29}$$

Solving for a, we define a new target semi-major axis, a^{**}, which forces the mean anomaly error to zero:

$$a^{**} = \left(-K_n \delta M + \frac{1}{a^{*3/2}} \right)^{-2/3} \tag{30}$$

Notice that as δM goes to zero, the mean motion control target semi-major axis, a^{**}, approaches the original target value, a^*. In application, we replace the mean anomaly error, δM, in Eq. (30) with argument of latitude error, $\delta\theta$, so that the mean motion control properly positions the spacecraft within the orbital plane, even in the presence of argument of periapse error.

Using the orbit control law defined in Eq. (24), with the target semi-major axis a^{**} defined in Eq. (30), we can control the full, nonlinear motion of an orbiting spacecraft. Since most spacecraft have fixed magnitude thrusters, we must develop some way of discretizing the control acceleration requested by the control laws. For example, if the orbital element feedback control law requests acceleration of magnitude A in the $\hat{\alpha}$ direction, we must determine whether or not to thrust, and if so, in what direction. This decision is straightforward for this elemental control law, as we have full scaling freedom in the choice of gains. We simply calculate a desired thrust direction and magnitude from the control law, and thrust if and only if the desired thrust magnitude is greater than the available thrust magnitude. Mathematically, this thruster on/off logic requests thrust in the $\hat{\alpha}$ direction if and only if $A > T/m$ where T is the available thrust magnitude, and m is the spacecraft mass.

In the case of the HokieSat mission, we not only scale the thrust magnitude, but also constrain the thrust direction. HokieSat's orbit control consists of four pulsed plasma

thrusters (PPTs) aligned in the local horizontal frame, with no thrust available in the radial direction. The classical orbital element Lyapunov control law can be modified to exclude radial thrusting by setting the terms in the first column of the **G** matrix in the control definition, Eq. (24), to zero, thus requesting only transverse and orbit normal thrust. By LaSalle's invariance principle, this modification does not affect the stability of the system, as the maximum invarient set for which $\dot{V} = 0$ remains $\boldsymbol{\eta} = \mathbf{0}$.

Orbit Control Gain Selection

Nonlinear feedback control gain selection techniques are described in Ref. 11. Following these guidelines, we choose the following positive feedback control gains to 1) guarantee asymptotic convergence to an error envelope, 2) appropriately weight the elemental errors, and 3) eliminate the problem of chattering by properly defining the size of the error envelope. These gains are calculated as functions of the target orbit elements in canonical units ($\mu = 1$, $DU = R_e$) as follows:

$$K_a = \frac{h^2}{4a^4(1+e)^2} \tag{31}$$

$$K_e = \frac{h^2}{4p^2} \tag{32}$$

$$K_i = \left[\frac{h + eh\cos\left(\omega + \arcsin(e\sin\omega)\right)}{p(-1+e^2\sin^2\omega)}\right]^2 \tag{33}$$

$$K_\Omega = \left[\frac{h\sin i(-1+e\sin\left(\omega + \arcsin(e\cos\omega)\right))}{p(1-e^2\cos^2\omega)}\right]^2 \tag{34}$$

$$K_\omega = \frac{e^2h^2}{4p^2}\left(1 - \frac{e^2}{4}\right) \tag{35}$$

We modify these feedback control gains by trigonometric functions of the true anomaly, ν, as suggested by Schaub and Alfriend:[18]

$$\tilde{K}_a = K_a \sin^N \nu \tag{36}$$

$$\tilde{K}_e = K_e \cos^N \nu \tag{37}$$

$$\tilde{K}_i = K_i \cos^N \theta \tag{38}$$

$$\tilde{K}_\Omega = K_\Omega \sin^N \theta \tag{39}$$

$$\tilde{K}_\omega = K_\omega \sin^N \nu \tag{40}$$

where N is some positive integer. Schaub *et al.*[18] suggest a slight variation of this form (with K_a multiplied by $\cos^N \nu/2$), to encourage control of the elements when they are the most controllable. For example, semi-major axis error would be emphasized at periapse, and mostly ignored elsewhere. The form given by Eq. (36) is more appropriate for HokieSat because it encourages control of δa not when a is most controllable, but when semi-major axis control will have the least impact on the eccentricity error. By not creating error in one element in the process of correcting error in another,[19] we can significantly reduce the fuel required to perform a given maneuver.

INTEGRATED ATTITUDE AND ORBIT CONTROL SIMULATION

To test the control laws, we apply them in a simulation of HokieSat's flight software. The test case is a rendezvous between a controlled spacecraft and an uncontrolled target orbit. The simulation is written in C++ and performed on a Linux machine. The simulation emulates the software environment that will run on HokieSat's onboard computer.

HokieSat will be controlled by an onboard computer running the VxWorks real-time operating system. The software architecture uses several processes running simultaneously. These processes can set global variables that other processes can read, and the processes can also send messages to one another. Each process controls a specific spacecraft subsystem; *e.g.*, there is a process that controls downlink communications to the ground station.

In these simulations, we model the software architecture that will be used onboard HokieSat. The simulations are performed in the Linux operating system, using a C++ library that simulates the VxWorks operating system. The simulation involves four processes, which interact in the same way that the flight processes interact. The four processes are Orbit Determination, Orbit Control, Attitude Determination, and Attitude Control. The intention is for each of the controls processes to resemble the flight code as much as possible. The attitude and orbit determination processes are simulated by numerical integrators, in place of the sensors that will be on HokieSat.

Orbit Determination Process

At each time step, the orbit determination process propagates the orbital position and velocity from the previous time to the current time. The propagation is performed using a 4th-order Runge-Kutta integrator. The only forces included are the two-body force and the applied thrust. Both orbits are propagated at each time step; the target orbit is integrated without any thrust, and the controlled orbit is integrated using the thrust direction calculated by the orbit control process in the previous time step. The magnitude of the thrust is 56 μN per thruster used, or zero if no thrust is applied. We assume a 20-kg spacecraft.

Attitude Determination Process

The attitude determination process propagates the attitude of the controlled spacecraft at each time step. The equations of motion for the attitude are integrated with a 4th-order Runge-Kutta integrator to find the current quaternion relating body and orbital frames, and the angular velocity, at the current time. Thrust and gravity gradient torques are considered, as well as the magnetic control torque calculated by the attitude control process at the previous time step.

Orbit Control Process

The orbital control process calculates the control thrust at each time step. It reads the current and desired (target) orbital positions and velocities, and determines the desired thrust direction based on the control law. Because HokieSat must remain nadir pointing, any radial component of the thrust direction determined by the control law is ignored and set to zero. If the control law determines a thrust magnitude that is less than the amount of

thrust that HokieSat can provide, then no thrust is applied. If the control law determines a thrust that is greater than the amount of thrust that HokieSat can provide, then the thrust magnitude is set equal to HokieSat's thrust. Based on the desired thrust direction, a desired attitude is determined in a quaternion form. This quaternion is compared to the current attitude quaternion calculated by the attitude determination process. If the attitude error is within 5°, and if the angular velocities are below 0.001 rad/sec, thrust is applied. When the thrust is applied, the thrust direction in the inertial frame is calculated by converting the thrust direction from the body frame to the inertial frame. This inertial thrust direction is then sent to the orbit determination task to use when propagating to the next time step. If the angle between the desired attitude and the current attitude is above the tolerance, or the angular velocities are above the tolerance, no thrust is performed, and the orbit control process sets the desired attitude for the attitude control process to read.

Attitude Control Process

At each time step, the attitude control process reads the current and desired attitudes and angular velocities, and calculates a torque based on the control law. If the calculated torque magnitude is above the maximum torque that HokieSat can provide, the torque is set equal to the maximum torque. If the orbital control process has not commanded a thrust, then the calculated torque is sent to the attitude determination process to use when propagating to the next time step. If the orbit control process has commanded a thrust, then the control torque is set to zero.

SIMULATION RESULTS

The initial conditions of the target orbit are defined by a 6770 km, nearly circular orbit with inclination of 52°. The initial conditions of the maneuvering spacecraft are dependent on the test case, and are either a 700 m position separation from the target, a 1 m/s velocity error from the target, or a combination of the two. In the simulations the initial attitude is chosen so that there is no initial attitude error. The initial angular velocity between the orbital and body frames is set to zero. The moment of inertia matrix, $\mathbf{I}$, used in the simulation, is based on a mass properties study performed at Wallops Flight Facility,[6] and is:

$$\mathbf{I} = \begin{bmatrix} 0.518 & 0.0046 & 0.0 \\ 0.0046 & 0.4898 & 0.0 \\ 0.0 & 0.0 & 0.4530 \end{bmatrix} \text{ kg m}^2 \tag{41}$$

We investigate several possibilities using these simulations. There are five types of cases to consider for simulations, each with varying degrees of fidelity as regards the actual system. First, the attitude control torque can either be the ideal torque or it can be constrained to the actual magnetic torque coil system that will be used in the satellite. The latter is of course the most important; however, simulations using the ideal torque aid in understanding of the overall system performance. Second, the orbit control strategy can use the normal mode or sideways mode. Third, the spacecraft can execute required controls throughout the orbit or the effects of eclipse can be included. For the eclipse mode, we assume as a worst case that eclipse lasts 45 minutes. Fourth, the initial position error (taken as 700 m) can be either in-track, cross-track, or radial, or a combination of the three. Fifth, the initial velocity error (taken as 1 m/s) can be in any direction.

Figure 2 shows the results of a leader-follower maneuver performed in the normal flight mode, with magnetic torque attitude control, and no eclipse eclipse constraint. The initial state of the maneuvering spacecraft in this simulation is defined by a 1×10^{-4} radian initial mean anomaly offset from the target orbit. Position error is reduced to < 10 m in less than one day. The convergence rate of position error is slow because the orbit control law requires frequent 180° attitude maneuvers but the available magnetic attitude control torque is small.

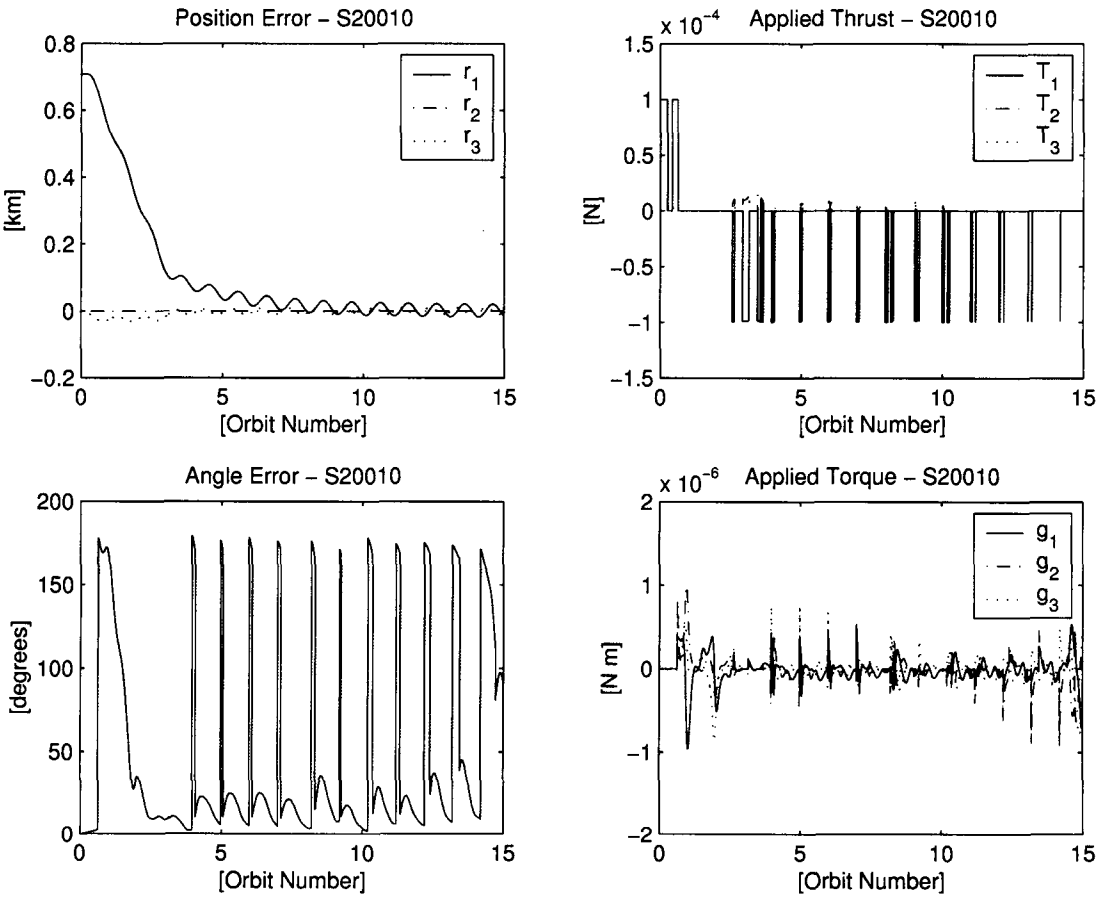

Figure 2: Simulation results for a 700-m leader-follower maneuver in the normal flight mode.

Figure 3 shows the results of a same-ground-track maneuver performed in the normal flight mode with magnetic attitude control, zero velocity error, and no eclipse. The initial state of the maneuvering spacecraft in this simulation is defined by a 1×10^{-4} radian initial mean anomaly offset, and a -1×10^{-5} radian initial right ascension offset from the target orbit. In this simulation, the control fails to complete the maneuver. This is due to the rapidly changing thrust direction, and the magnetic attitude control subsystem's inability to promptly point the thrusters in the required direction.

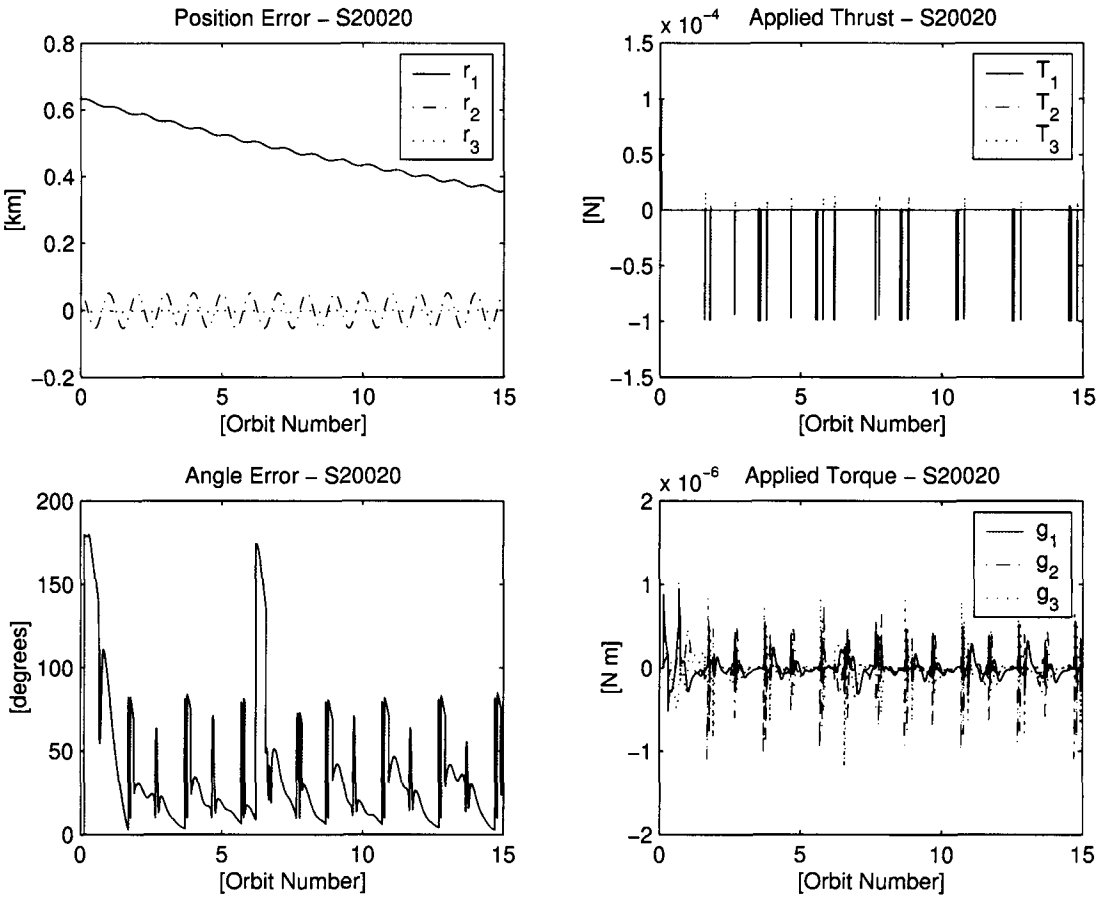

Figure 3: Simulation results for a 700-m same ground track maneuver in the normal flight mode.

This problem due to the attitude control by the magnetic torque coil can be overcome by the sideways flight mode. Figure 4 shows a 700-m same ground track maneuver, respectively, in the sideways flight mode with the magnetic torque attitude control. The convergence rate of position error is much faster than the previous case because this mode does not require a large angle attitude maneuver.

Considering the effects of eclipse has further impact on performance. In Figure 5, the eclipse lasts for a half orbit period per each orbit. This trajectory uses sideways mode, in-track position error, magnetic attitude control, and no velocity error. The convergence rate is slightly slower than the no eclipse case but not by much. Attitude control during the eclipse allows the orbit control to perform effectively immediately after eclipse.

Figure 6 shows simulations results with initial velocity errors. When the initial velocity error is large enough, it is difficult to overcome these errors using a limited power thruster, especially if the velocity error is in the orbital velocity direction (Figure 6(a)). It takes hundreds of orbits to be able to observe convergence. When considering eclipse, it takes

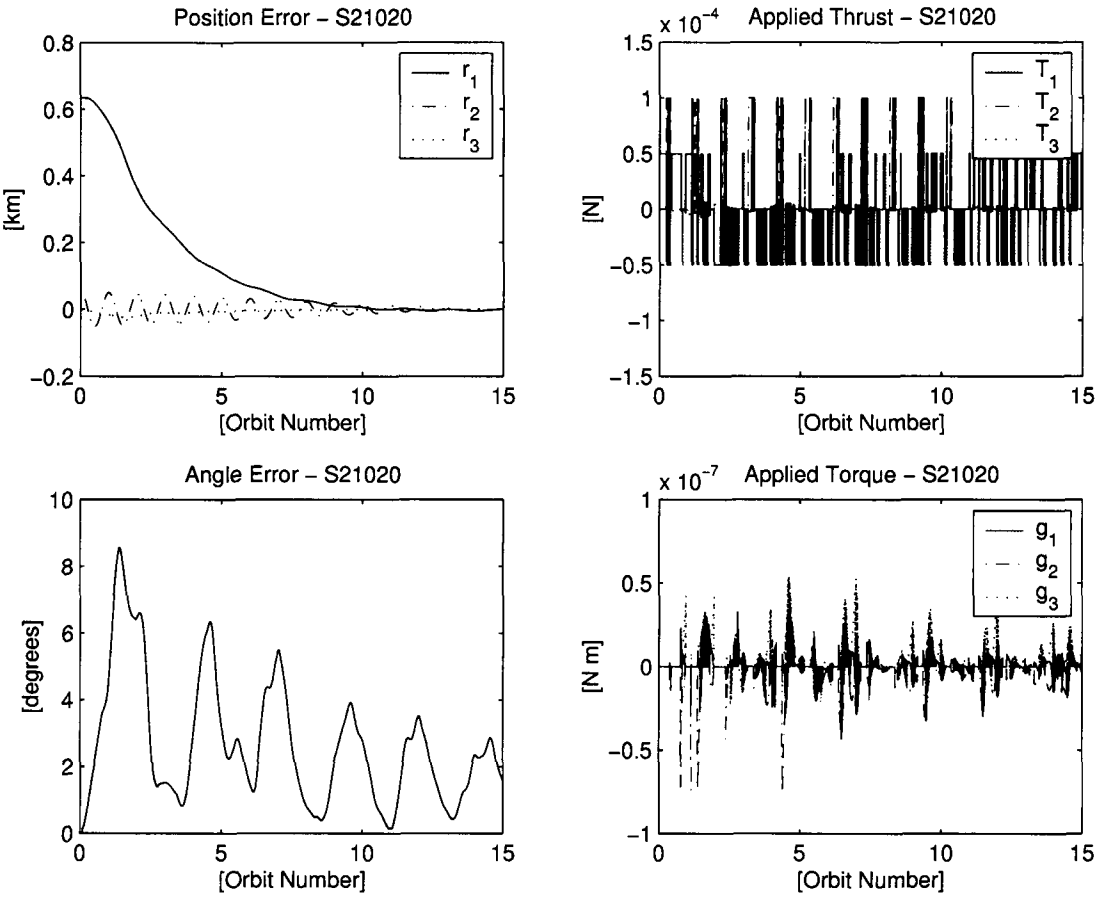

Figure 4: Simulation results for a 700-m same ground track maneuver in the sideways flight mode.

twice as long to achieve convergence. This result implies a significant emphasis should be placed on insuring that initial velocity errors due to spacecraft separation are minimized.

CONCLUSIONS

Attitude and orbit control systems are frequently considered to be independent. However, in small spacecraft with limited power, the coupling can be significantly greater if control actuators cannot be used simultaneously. Further performance degradation results if actuators cannot be used during eclipse. Independently developed controllers can be successfully integrated to achieve reasonable performance, as illustrated by the simulation results presented in this paper. The HokieSat mission has limited power, limited thrust magnitude, fixed thrust direction, no thrust during eclipse, and limited attitude control torque. A successful control strategy uses orbit element feedback for orbit control, and a modified LQR-based control for attitude control. To avoid the problems of frequent direction changes in the re-

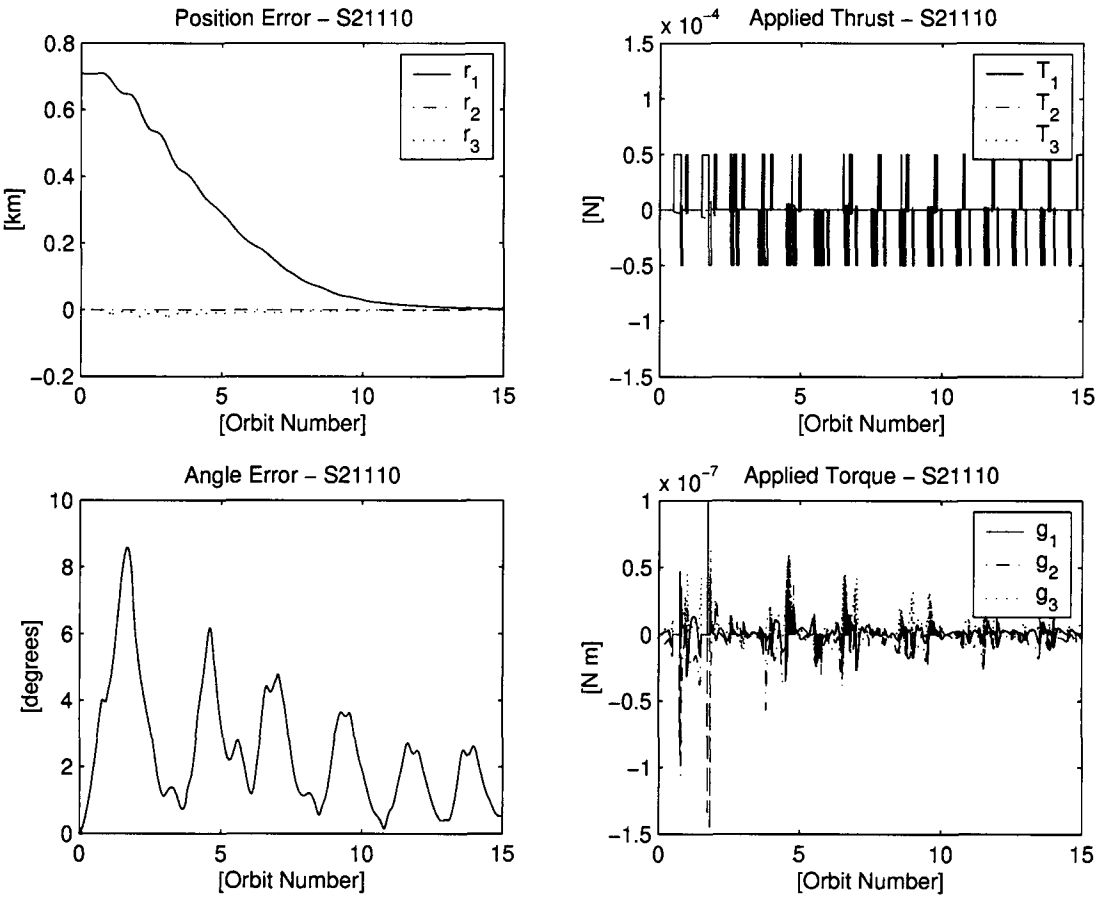

Figure 5: Simulation results for a 700-m leader-follower maneuver in the sideways flight mode with eclipse.

quired thrust, the spacecraft flies "sideways" so that thrust can be applied in the $\pm$ velocity direction. Effects of initial velocity and position errors can be substantial.

REFERENCES

[1] Hughes, P. C., *Spacecraft Attitude Dynamics*, John Wiley & Sons, New York, 1986.

[2] Beck, J. A. and Hall, C. D., "Relative Equilibria of a Rigid Satellite in a Circular Keplerian Orbit," *Journal of the Astronautical Sciences*, Vol. 46, No. 3, 1998, pp. 215–247.

[3] Hall, C. D. et al., "Virginia Tech Ionospheric Scintillation Measurement Mission," *Proceedings of the AIAA/Utah State University Conference on Small Satellites*, Logan, Utah, Aug 1999.

[4] Campbell, M., Fullmer, R. R., and Hall, C. D., "The ION-F Formation Flying Experiments," *Proceedings of the 2000 AAS/AIAA Space Flight Mechanics Meeting*, Clearwater, Florida, Jan 2000.

[5] Stevens, C. L., Schwartz, J. L., and Hall, C. D., "Design and System Identification of a Nanosatellite Structure," *Proceedings of the 2001 AAS/AIAA Astrodynamics Specialists Conference*, Quebec City, Quebec, 2001.

[6] Stevens, C. L., *Design, Analysis, Fabrication and Testing of a Nanosatellite Structure*, Master's thesis, Virginia Polytechnic Institute and State University, Blacksburg, Virginia, 2002.

[7] Makovec, K. L., Turner, A. J., and Hall, C. D., "Design and Implementation of a Nanosatellite Attitude Determination and Control System," *Proceedings of the 2001 AAS/AIAA Astrodynamics Specialists Conference*, Quebec City, Quebec, 2001.

[8] Makovec, K. L., *A Nonlinear Magnetic Controller for Nanosatellite Applications*, Master's thesis, Virginia Polytechnic Institute and State University, Blacksburg, Virginia, 2001.

[9] Turner, A. J. and Hall, C. D., "Adaptive Spacecraft Attitude Control Using Neural Networks," *Proceedings of the Virginia Space Grant Consortium Student Research Conference*, Hampton, Virginia, March 2002.

[10] Naasz, B. J., Karlgaard, C. D., and Hall, C. D., "Application of Several Control Techniques for the Ionospheric Observation Nanosatellite Formation," *Proceedings of the 2002 AAS/AIAA Space Flight Mechanics Meeting*, San Antonio, Texas, Jan 2002.

[11] Naasz, B. J. and Hall, C. D., "Classical Element Feedback Control for Spacecraft Orbital Maneuvers," *Journal of Guidance, Control and Dynamics*, 2002, submitted.

[12] Naasz, B. J., *Classical Element Feedback Control for Spacecraft Orbital Maneuvers*, Master's thesis, Virginia Polytechnic Institute and State University, Blacksburg, Virginia, 2002.

[13] Hall, C. D. and Collazo Perez, V., "Minimum-Time Orbital Phasing Maneuvers," *Journal of Guidance, Control and Dynamics*, 2002, submitted.

[14] Hall, C. D. and Collazo Perez, V., "Minimum-Time Orbital Phasing Maneuvers," *Proceedings of the 2003 AAS/AIAA Space Flight Mechanics Meeting*, Ponce, Puerto Rico, Feb 2003.

[15] Cassady, R. J., Hoskins, A. W., Campbell, M., and Rayburn, C., "A Micro-Pulsed Plasma Thruster for the Dawgstar Spacecraft," *Proceedings of the 2000 IEEE Aerospace Conference*, Big Sky, Montana, 2000.

[16] Rayburn, C., Campbell, M., Hoskins, A. W., and Cassady, R. J., "Development of a Micro-PPT for the Dawgstar Nanosatellite," *Proceedings of the 2000 AIAA/ASME/SAE/ASEE Joint Propulsion Conference*, Huntsville, Alabama, 2000.

[17] Battin, R. H., *An Introduction to the Mathematics and Methods of Astrodynamics, Revised Edition*, American Institute of Aeronautics and Astronautics, Inc, Reston, VA, 1999.

[18] Schaub, H., Vadali, S. R., Junkins, J. L., and Alfriend, K. T., "Spacecraft Formation Flying Control Using Mean Orbital Elements," *Advances in the Astronautical Sciences*, Vol. 103, Part 1, 1999, pp. 163–181, AAS 99-310.

[19] Schaub, H. and Alfriend, K. T., "Impulsive Spacecraft Formation Flying Control to Establish Specific Mean Orbit Elements," *Journal of Guidance, Control, and Dynamics*, Vol. 24, No. 4, 2001, pp. 739–745.

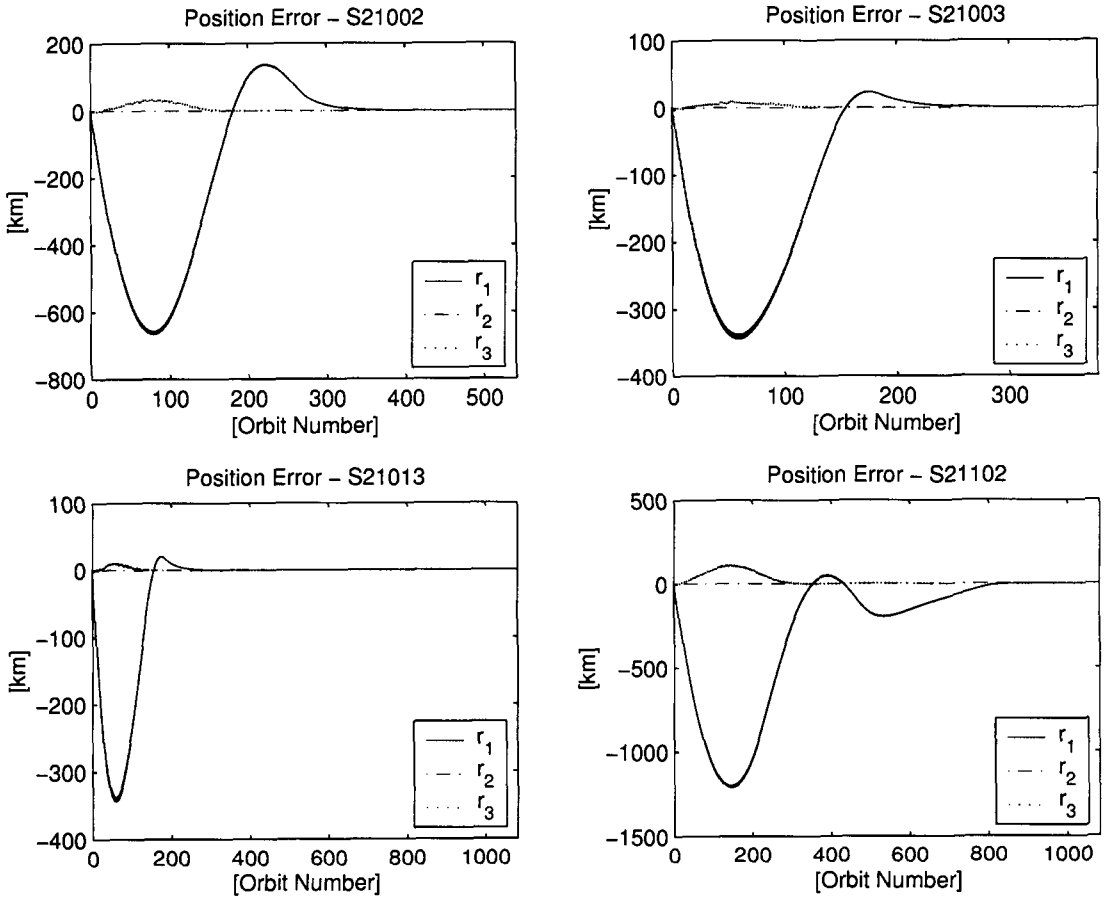

Figure 6: Simulation results for initial velocity errors (1m/sec) in the sideways flight mode (a) $\hat{\mathbf{o}}_1$-axis direction error - S21002, (b) random direction velocity error - S21003, (c) position and random direction velocity error - S21013, (d) $\mathbf{o}_1$-axis direction error with eclipse - S21102.